

Mechanistic Importance of Intermediate $N_2O + CO$ Reaction in Overall $NO + CO$ Reaction System

I. Kinetic Analysis

BYONG K. CHO

*Physical Chemistry Department, General Motors Research and Environmental Staff,
Warren, Michigan 48090-9055*

Received January 20, 1992; revised May 26, 1992

To investigate the mechanistic importance of the $N_2O + CO$ reaction as an intermediate reaction step during the reduction of NO by CO occurring on noble metal exhaust catalysts, we have analyzed theoretically the steady-state kinetics of the $NO + CO$ reaction based on elementary surface processes. Quasilinearization of the nonlinear $NO + CO$ reaction system by identifying a critical kinetic parameter has enabled us to develop a complete set of analytical solutions for the system which includes the intermediate $N_2O + CO$ reaction step. The kinetic analysis based on this solution scheme shows a dramatic difference between the rate of the $N_2O + CO$ reaction as an *intermediate* reaction and that as an *isolated* reaction. Results have revealed that the rate of the $N_2O + CO$ reaction as an intermediate reaction in the $NO + CO$ reaction system can be two to three orders of magnitude faster than the isolated $N_2O + CO$ reaction, which is known to be very slow compared with the $NO + CO$ reaction. This makes the rate of the intermediate $N_2O + CO$ reaction as fast as or even faster than the rate of the $NO + CO$ reaction, suggesting that the former reaction can make a major contribution to the kinetics of the reduction of NO by CO occurring in three-way catalytic converters. © 1992 Academic Press, Inc.

INTRODUCTION

There are at least two reasons why efficient removal of NO in the catalytic converter is important. Obviously, the removal of NO is important from an emission-control point of view. Not quite so obvious, it is also important from the kinetic point of view, because the presence of NO is known to inhibit the catalytic oxidation of CO and hydrocarbons by oxygen on noble metal catalysts (1, 2). Thus, a clear understanding of the detailed reaction mechanism involved in the NO reduction process is of practical significance as well as fundamental importance for automotive exhaust emission control.

Reduction of NO by CO is one of the most important catalytic reactions occurring in automobile catalytic converters to remove NO from the engine exhaust. Rhodium is widely recognized as the most efficient cata-

lytic component to promote the reduction of NO to N_2 in three-way catalysts (3). The mechanism of this reaction on noble metal catalysts, especially on Rh catalysts, appears to be reasonably well understood as a result of the extensive research efforts during the past decade or so (e.g., 4-12). However, it is not until recently that we have come to recognize the participation of $N_2O + CO$ reaction as an intermediate reaction step during the overall $NO + CO$ reaction (11). In this regard, it is interesting to note that Hecker and Bell (7) observed the formation of N_2O during the $NO + CO$ reaction over Rh/SiO_2 , but they reported no measurable activity of Rh/SiO_2 for the further reduction of N_2O by CO , in disagreement with the later findings by Cho *et al.* over Rh/Al_2O_3 and Rh/CeO_2 (11).

More recently, McCabe and Wong (13) in their study of the $N_2O + CO$ reaction kinetics over an Rh/Al_2O_3 catalyst have con-

firmed the findings by Cho *et al.* (11) regarding the participation of $N_2O + CO$ reaction as an important subreaction in the overall $NO + CO$ reaction system. However, their results have revealed that the rate of the $N_2O + CO$ reaction is about two orders of magnitude slower than that of the $NO + CO$ reaction, in accordance with the earlier findings by Hecker and Bell (7). The slow rate of the $N_2O + CO$ reaction compared with the rate of the $NO + CO$ reaction was attributed to slow N_2O decomposition caused by the strong CO inhibition effect, which has been confirmed lately by Belton and Schmiegel (14). These latest findings suggest that the kinetic contribution of the $N_2O + CO$ reaction to the overall $NO + CO$ reaction system should be negligible due to the very slow rate of the $N_2O + CO$ reaction. This in turn implies that the $N_2O + CO$ reaction as an intermediate reaction step during the $NO + CO$ reaction can be safely assumed to be negligible, possibly justifying the omission of the $N_2O + CO$ reaction in the interpretation of the overall $NO + CO$ reaction system (7, 10). One of the objectives of this paper is to examine whether this logic is well justified.

In assessing the implications of the above findings in the kinetic analysis of the $NO + CO$ reaction system, it is important to recognize that the above studies on the $N_2O + CO$ reaction kinetics (13, 14) were carried out as an isolated reaction system, not as an intermediate reaction step occurring in the overall $NO + CO$ reaction system. As shown in this paper, the rate of the $N_2O + CO$ reaction as an intermediate reaction step in the overall $NO + CO$ reaction system can be much faster than the rate of the isolated $N_2O + CO$ reaction. In this work, we clarify, through kinetic analysis, the origin of this difference between the isolated reaction system and the overall reaction system.

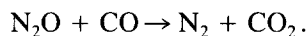
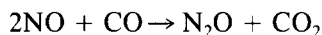
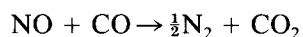
KINETIC ANALYSIS

The purpose of the detailed kinetic analysis presented in this section is to compare the rate of the $N_2O + CO$ reaction as an

isolated reaction system with that as an intermediate reaction in the overall $NO + CO$ reaction system. The latter we refer to as an overall reaction system. Since the steady-state rate of the $N_2O + CO$ reaction is limited by the rate of N_2O decomposition on the catalyst surface, it is appropriate to compare the rates of the $N_2O + CO$ reaction in terms of the rates of N_2O decomposition in both systems. Furthermore, since the decomposition rate of N_2O is of first order with respect to the surface coverage of N_2O (13) and the decomposition rate constant can be considered to be the same for both systems, the task of comparing the N_2O decomposition rate can be accomplished simply by comparing the surface coverage of N_2O between the two systems.

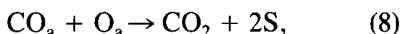
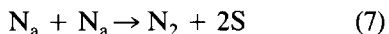
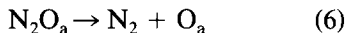
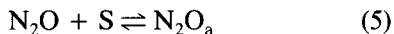
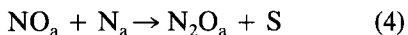
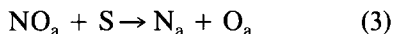
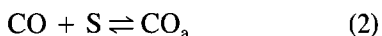
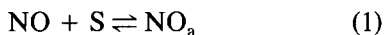
Kinetic Analysis of the Overall $NO + CO$ Reaction System

The overall $NO + CO$ reaction system involves the following three reaction pathways (11):



Since the isolated $N_2O + CO$ reaction system can be considered as a subset of the overall $NO + CO$ reaction system in which the $N_2O + CO$ reaction occurs as an intermediate reaction step, we focus on the overall $NO + CO$ reaction system first. Then the case of the isolated system follows naturally as a degenerate case of the overall system.

The mechanistic model presented below was developed by extending the surface chemistry model previously reported in the literature (7, 10) to include all the kinetic processes involving the adsorbed state of N_2O (11). Such a model provides a convenient means of examining the mechanistic importance of the intermediate $N_2O + CO$ reaction in the overall $NO + CO$ reaction system. Our model includes the sequence of elementary surface processes (11):



where the subscript "a" denotes adsorbed state. Note that Eqs. (4), (5), and (6) describe all the kinetic processes involving N₂O_a on the catalytic surface. Formation of isocyanate species (NCO) is not included in the model since it is known that the NCO species present on the Rh surface does not significantly affect the kinetics of the NO + CO reaction (8, 15). Based on the surface reaction mechanism listed above, the steady-state mass balance equations for the surface species NO_a, CO_a, N₂O_a, N_a, and O_a can be written as

$$k_1 C_{\text{NO}} \theta_v - k_{-1} \theta_{\text{NO}} - k_3 \theta_{\text{NO}} \theta_v - k_4 \theta_{\text{N}} \theta_{\text{NO}} = 0 \quad (9)$$

$$k_2 C_{\text{CO}} \theta_v - k_{-2} \theta_{\text{CO}} - k_8 \theta_{\text{CO}} \theta_{\text{O}} = 0 \quad (10)$$

$$k_4 \theta_{\text{N}} \theta_{\text{NO}} + k_5 C_{\text{N}_2\text{O}} \theta_v - k_{-5} \theta_{\text{N}_2\text{O}} - k_6 \theta_{\text{N}_2\text{O}} = 0 \quad (11)$$

$$k_3 \theta_{\text{NO}} \theta_v - k_4 \theta_{\text{N}} \theta_{\text{NO}} - 2k_7 \theta_{\text{N}}^2 = 0 \quad (12)$$

$$k_3 \theta_{\text{NO}} \theta_v + k_6 \theta_{\text{N}_2\text{O}} - k_8 \theta_{\text{CO}} \theta_{\text{O}} = 0, \quad (13)$$

where the surface vacancy θ_v can be approximated by

$$\theta_v = 1 - \theta_{\text{NO}} - \theta_{\text{CO}} - \theta_{\text{N}_2\text{O}} - \theta_{\text{N}}. \quad (14)$$

Note in Eq. (14) that the surface coverage of oxygen (θ_{O}) was assumed to be negligible because the rate of O_a consumption via CO oxidation is much faster than the rate of O_a production via NO_a and/or N₂O_a dissociation (10, 13).

Important kinetic parameters necessary for steady-state analysis of the NO + CO

reaction are listed in Table 1. Note that the activation energy for N₂O desorption used by McCabe and Wong (13) is in line with the value for Pt(111) reported by Avery (17) and that the two kinetic parameters k_4 and k_8 which appeared in the mass balance equations above are not required for the steady-state analysis, as shown later. Comparison of ε_{CO} and ε_{N} in Table 1 indicates that the activation energy of CO desorption is dependent on nitrogen coverage, whereas the activation energy of nitrogen desorption is independent of CO coverage. In other words, the repulsive interaction between N_a and CO_a on the surface facilitates the CO desorption, but not the nitrogen desorption. This seemingly counterintuitive phenomenon has been observed experimentally (9) and can be explained by the difference in desorption temperature between CO and nitrogen.

Since there is no literature data available for the sticking coefficient of N₂O on supported Rh surfaces, it is appropriate to elaborate on it which we have estimated to be 0.002. Dissociative adsorption on N₂O is known to be kinetically controlled by the molecular precursor state of N₂O which requires more restrictive surface sites than the molecular precursor state of O₂ (18, 19). In case of O₂ adsorption on the surface where CO is the dominating surface species, the dissociative sticking coefficient of O₂ becomes two orders of magnitude smaller than that on a clean surface due to the restrictive site requirements for the precursor state (10, 20). In view of these observations, it appears reasonable to reduce the value of the sticking coefficient of N₂O by at least two orders of magnitude from the literature value reported on clean surfaces (18, 21), when the surface is dominated by CO_a and/or N_a, as shown later. This gives an estimated value of 0.002 for the sticking coefficient of N₂O, which is in line with those reported for Pt surfaces (22, 23). Our own kinetic analysis of McCabe and Wong's data (13), which will be reported in a subsequent paper, has

TABLE I
Important Kinetic Parameters for Steady-State Analysis

Parameter	Used in this work	References
k_1 [(cm ³ /mol) s ⁻¹]	$\sigma S_{\text{NO}} f_{\text{NO}}$	(10)
k_{-1} (s ⁻¹)	$5 \times 10^{13} \exp(-26,000/R_g T)$	(10)
k_2 [(cm ³ /mol) s ⁻¹]	$\sigma S_{\text{CO}} f_{\text{CO}}$	(10, 13)
k_{-2} (s ⁻¹)	$1.6 \times 10^{14} \exp\{(-31,600 + \epsilon_{\text{CO}})/R_g T\}$	(10)
k_3 (s ⁻¹)	$6 \times 10^{13} \exp(-19,000/R_g T)$	(10)
k_5 [(cm ³ /mol) s ⁻¹]	$\sigma S_{\text{N}_2\text{O}} f_{\text{N}_2\text{O}}$	(13)
k_{-5} (s ⁻¹)	$1 \times 10^{13} \exp(-5000/R_g T)$	(13)
k_6 (s ⁻¹)	$2.6 \times 10^{13} \exp(-18,000/R_g T)$	(13)
k_7 (s ⁻¹)	$3 \times 10^{10} \exp\{(-31,000 + \epsilon_{\text{N}})/R_g T\}$	(10)
σ (cm ² /mol)	1.6×10^{15}	(13)
S_{NO}	0.5	(10)
S_{CO}	0.5	(10, 13)
$S_{\text{N}_2\text{O}}$	0.002	(estimated)
f_i (cm/s)	$[R_g T / (2\pi M_i)]^{0.5}$	(16)
ϵ_{CO} (cal/mol)	$4,500\theta_{\text{CO}} + 10,000\theta_{\text{N}}$	(10)
ϵ_{N} (cal/mol)	$4,000\theta_{\text{N}}$	(10)

indicated that the sticking coefficient of N₂O can be much smaller than 0.002 under reaction conditions of the (N₂O + CO) system. Thus, the above estimated value appears to be an appropriate upper bound for $S_{\text{N}_2\text{O}}$.

*Quasilinearization through
Nondimensional Parameterization*

For the present kinetic analysis, it is convenient to introduce dimensionless gas-phase concentrations

$$\Gamma_A = \alpha K_{\text{NO}} C_{\text{NO}}, \quad \Gamma_B = K_{\text{CO}} C_{\text{CO}}, \\ \Gamma_C = \beta K_{\text{N}_2\text{O}} C_{\text{N}_2\text{O}}, \quad (15)$$

and dimensionless parameters

$$K_{\text{NO}} = k_1/k_{-1}, \quad K_{\text{CO}} = k_2/k_{-2}, \\ K_{\text{N}_2\text{O}} = k_5/k_{-5}, \quad (16)$$

$$\alpha = k_{-1}/k_{-2}, \quad \beta = k_{-5}/k_{-2}, \\ \gamma = k_3/k_{-2}, \quad \delta = k_7/k_{-2}, \quad (17)$$

$$r_1 = \gamma\theta_{\text{v}}, \quad r_2 = k_6/k_{-2}. \quad (18)$$

A linear combination of Eqs. (9), (10), (11), and (13) then yields

$$\left(1 - \frac{\alpha}{\Gamma_B - \Gamma_A - \Gamma_C}\right) \theta_{\text{NO}} \\ - \left(1 + \frac{1}{\Gamma_B - \Gamma_A - \Gamma_C}\right) \theta_{\text{CO}} \\ + \left(1 - \frac{\beta}{\Gamma_B - \Gamma_A - \Gamma_C}\right) \theta_{\text{N}_2\text{O}} \\ + \theta_{\text{N}} = 1. \quad (19)$$

Similarly, another linear combination of Eqs. (10) and (13) yields

$$\left(1 + \frac{r_1}{\Gamma_B}\right) \theta_{\text{NO}} + \left(1 + \frac{1}{\Gamma_B}\right) \theta_{\text{CO}} \\ + \left(1 + \frac{r_2}{\Gamma_B}\right) \theta_{\text{N}_2\text{O}} + \theta_{\text{N}} = 1, \quad (20)$$

while that of Eqs. (9) and (12) results in

$$\left(1 + \frac{\alpha}{2\Gamma_C + \Gamma_A}\right) \theta_{\text{NO}} + \theta_{\text{CO}} \\ + \left(1 + \frac{2\beta + 2r_2}{2\Gamma_C + \Gamma_A}\right) \theta_{\text{N}_2\text{O}} + \theta_{\text{N}} \\ = 1 - \left(\frac{2\delta\theta_{\text{N}}^2}{2\Gamma_C + \Gamma_A}\right). \quad (21)$$

For further analysis, it is useful to recog-

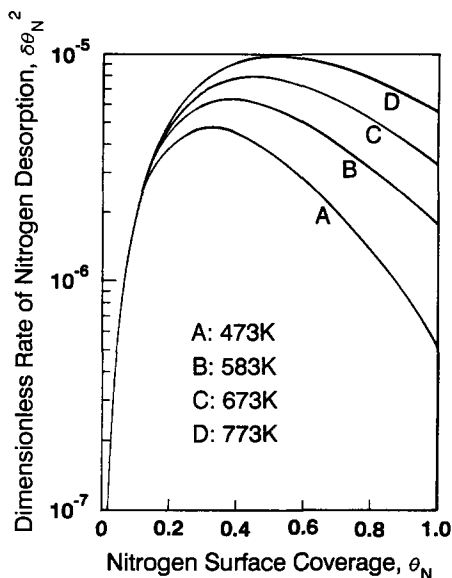


FIG. 1. Dimensionless rate of nitrogen desorption via nitrogen atom recombination as a function of nitrogen surface coverage.

nize in Eq. (21) that $\delta \theta_N^2$ is extremely small over all possible values of θ_N , as can be seen in Fig. 1, which was calculated using the kinetic parameters listed in Table 1. In estimating δ , we assumed as a conservative measure that θ_{CO} is zero on the Rh surface.

$$\mathbf{M} = \begin{pmatrix} 1 - \alpha/(\Gamma_B - \Gamma_A - \Gamma_C) & 1 + 1/(\Gamma_B - \Gamma_A - \Gamma_C) & 1 - \beta/(\Gamma_B - \Gamma_A - \Gamma_C) & 1 \\ 1 + r_1/\Gamma_B & 1 + 1/\Gamma_B & 1 + r_2/\Gamma_B & 1 \\ 1 + \alpha/(2\Gamma_C + \Gamma_A) & 1 & 1 + 2(\beta + r_2)/(2\Gamma_C + \Gamma_A) & 1 \end{pmatrix} \quad (24)$$

$$\Theta = [\theta_{\text{NO}} \theta_{\text{CO}} \theta_{\text{N}_2\text{O}} \theta_{\text{N}}]^T \quad (25)$$

$$\mathbf{H} = [1 \ 1 \ 1]^T. \quad (26)$$

Solving Eq. (23) in terms of θ_{N} assuming the matrix \mathbf{M} is a constant matrix (i.e., all its elements are constant) (24), we get

$$\frac{\theta_{\text{NO}}}{1 - \theta_{\text{N}}} = (\beta + r_2)\Gamma_A/D, \quad (27)$$

$$\frac{\theta_{\text{CO}}}{1 - \theta_{\text{N}}} = \{(\alpha + 2r_1)(\beta + r_2)\Gamma_B - r_1(\beta + 2r_2)\Gamma_A - r_2(\alpha + 2r_1)\Gamma_C\}/D, \quad (28)$$

That is, the actual value of δ can be much smaller than what we estimated it to be if the actual θ_{CO} is nonzero. Under the circumstances, the second term on the right-hand side of Eq. (21) can safely be ignored since the magnitude of $(2\Gamma_C + \Gamma_A)$ is typically on the order of unity as will be shown later. That is,

$$\frac{2\delta\theta_{\text{N}}^2}{2\Gamma_C + \Gamma_A} \approx 0. \quad (22)$$

Steady-State Surface Coverage of Reacting Species

It is important to note in the above formulation that the parameter r_1 is not a constant parameter because it is a function of θ_{v} , which is in turn a function of θ_{NO} , θ_{CO} , $\theta_{\text{N}_2\text{O}}$, and θ_{N} through Eq. (14). For the moment, however, we can treat r_1 as a constant parameter whose value is to be determined later in such a way that Eq. (14) is satisfied. In this sense, we call it *optimization parameter*. With this idea of the optimization parameter (r_1) along with the help of Eq. (22), the three equations (19), (20), and (21) can be represented by a system of quasilinear equations in a maxtrix form such as

$$\mathbf{M}\Theta = \mathbf{H}, \quad (23)$$

where

$$\frac{\theta_{\text{N}_2\text{O}}}{1 - \theta_{\text{N}}} = \{(\alpha + 2r_1)\Gamma_C + r_1\Gamma_A\}/D, \quad (29)$$

where

$$D = (\alpha + 2r_1)\{(\beta + r_2)(1 + \Gamma_B) + (1 - r_2)\Gamma_C\} - \{(r_1 - 1)(\beta + 2r_2 - 1) + r_2 - 1\}\Gamma_A. \quad (30)$$

Transforming the right-hand side of Eqs.

(27) through (29) into the same form as their left-hand side, we can express the steady-state surface coverages in terms of r_1 as

$$\theta_N = \{(r_1 - 1)(\beta + 2r_2 - 1) + r_2 - 1\}\Gamma_A/\{(\alpha + 2r_1)\Delta\}, \quad (31)$$

$$\theta_{NO} = (\beta + r_2)\Gamma_A/\{(\alpha + 2r_1)\Delta\}, \quad (32)$$

$$\theta_{CO} = \{(\alpha + 2r_1)(\beta + r_2)\Gamma_B - r_1(\beta + 2r_2)\Gamma_A - r_2(\alpha + 2r_1)\Gamma_C\}/\{(\alpha + 2r_1)\Delta\}, \quad (33)$$

$$\theta_{N_2O} = \{(\alpha + 2r_1)\Gamma_C + r_1\Gamma_A\}/\{(\alpha + 2r_1)\Delta\}, \quad (34)$$

where Δ is the inhibition function which characterizes the inhibition effect due to the adsorbed CO and N_2O species on the catalytic surface and is defined by

$$\Delta = (\beta + r_2)(1 + \Gamma_B) + (1 - r_2)\Gamma_C. \quad (35)$$

As will become more apparent in later discussions, the inhibition function Δ provides a common ground on which to compare the surface coverages of reacting species in the NO + CO reaction system with those in the N_2O + CO reaction system. Equations (31) through (34) constitute part of the complete set of solutions for the steady-state surface coverages of the reacting species in the (NO + CO) reaction system. It is important to note here that the optimization parameter r_1 —which is a function of θ_v by its definition—has yet to be determined in such a way that Eq. (14) is satisfied as follows.

Determination of the optimization parameter r_1 . Since θ_{NO} , θ_{CO} , θ_{N_2O} , θ_N , and θ_v are all functions of r_1 , we can use Eq. (14) as the optimization condition for r_1 . Thus, inserting Eqs. (31) through (34) into Eq. (14) we get

$$ar_1^2 + br_1 + c = 0, \quad (36)$$

where

$$a = 2\Delta/\gamma, \quad b = \alpha\Delta/\gamma - 2(\beta + r_2), \\ c = -\alpha(\beta + r_2). \quad (37)$$

The positive solution of Eq. (36),

$$r_1 = \gamma(\beta + r_2)/\Delta, \quad (38)$$

is the optimized value of r_1 to be used in Eqs. (31) through (34) to determine θ_{NO} , θ_{CO} , θ_{N_2O} , and θ_N . From Eq. (38) and the definition of r_1 , we get

$$\theta_v = (\beta + r_2)/\Delta. \quad (39)$$

Thus, Eqs. (31) through (34), and Eqs. (38) and (39) are the complete set of analytical solutions for the steady-state surface coverages of the reacting species in the NO + CO reaction system. This solution provides a convenient way to compare the kinetics of the isolated N_2O + CO reaction with that of the intermediate N_2O + CO reaction in the overall NO + CO system.

Rate of N_2O + CO Reaction as an Isolated System

In an isolated N_2O + CO reaction system, both NO_a and N_a are absent since N_2O dissociation on noble metal surfaces is known to occur via $N_2O_a \rightarrow N_2 + O_a$ (13, 18–20). That is,

$$\Gamma_A = 0, \quad \theta_{NO} = 0, \quad \text{and} \quad \theta_N = 0. \quad (40)$$

Equations (33) and (34) can then be reduced to

$$\theta_{CO} = \{(\beta + r_2)\Gamma_B - r_2\Gamma_C\}/\Delta, \quad (41)$$

$$\theta_{N_2O} = \Gamma_C/\Delta, \quad (42)$$

$$\theta_v = (\beta + r_2)/\Delta, \quad (43)$$

for the isolated N_2O + CO reaction system. Note a slight difference between Eq. (42) above and Eq. (A.5) in McCabe and Wong (13); the inhibition function (Δ) in their expression becomes $\{(\beta + r_2)(1 + \Gamma_B) - r_2\Gamma_C\}$ instead of being the same as that in Eq. (35). This difference is due to the latter authors' assumption of negligible contribution by θ_{N_2O} to the total surface coverage. Though their assumption is quite reasonable for their particular experimental conditions, our results clearly show that it is an unnecessary assumption. It is remarkable to see by comparing Eqs. (39) and (43) that θ_v is expressed in exactly the same form for both systems.

Under steady-state conditions, the rate of the N₂O + CO reaction is equal to the rate of N₂O decomposition. Thus, the rate of the isolated N₂O + CO reaction (R_i) can be expressed as

$$R_i = k_6\theta_{N_2O} = k_6\Gamma_C/\Delta. \quad (44)$$

Rate of N₂O + CO Reaction in an Overall NO + CO Reaction System

With the aid of Eq. (34), the rate of the N₂O decomposition in the overall NO + CO reaction system (R_o) can be written as

$$R_o = k_6\theta_{N_2O} = k_6 \left(\Gamma_C + \frac{r_1\Gamma_A}{\alpha + 2r_1} \right) / \Delta. \quad (45)$$

Comparison of the Rate of N₂O + CO Reaction: Isolated System vs Overall System

Comparison of Eq. (44) with Eq. (45) reveals that the rate of the N₂O + CO reaction in the overall NO + CO reaction system [Eq. (45)] can be much faster than the rate of the isolated N₂O + CO reaction [Eq. (44)]. The rate-enhancement factor (η), defined as the ratio of R_o to R_i , can be written as

$$\eta = \frac{R_o}{R_i} = \left(\frac{\Gamma_{C,o} + r_1\Gamma_{A,o}/(\alpha + 2r_1)}{\Gamma_{C,i}} \right) \frac{\Delta_i}{\Delta_o}, \quad (46)$$

where subscripts *i* and *o* stand for the isolated N₂O + CO system and for the overall NO + CO system, respectively. As shown later Δ_i and Δ_o are not the same, in general, due to different repulsive interactions among adsorbed species on the surface. It is useful to note here that the gas-phase concentration of N₂O during the NO + CO reaction is always smaller than the feed concentration of NO and is negligibly small except at low temperatures (11, 13). This suggests that Eq. (46) can be approximated by

$$\eta = \left(\frac{r_1}{\alpha + 2r_1} \right) \left(\frac{\Gamma_{A,o}}{\Gamma_{C,i}} \right) \left(\frac{\Delta_i}{\Delta_o} \right) \quad (47)$$

TABLE 2

Dimensionless Parameter Values Calculated from Table 1 (583 K)

Parameter	Calculated value at 583 K	
	Isolated system	Overall system
α	—	4.667×10^{-1}
β	1.914×10^6	6.932×10^5
r_1	—	6.451×10
r_2	6.711×10^3	2.431×10^3
Γ_A	—	2.560
Γ_B	7.313	2.650
Γ_C	2.334×10^{-2}	8.454×10^{-3}
Δ	1.591×10^8	2.531×10^7
ϵ_{CO} (cal/mol)	3.959×10^3	5.135×10^3

Note. $C_{CO} = C_{N_2O} = 400$ ppm was used for the isolated system; $C_{NO} = C_{CO} = C_{N_2O} = 400$ ppm was used for the overall system.

by neglecting the contribution of $\Gamma_{C,o}$ to the rate-enhancement factor.

In determining the rate-enhancement factor using Eq. (46) or (47), it is important to recognize that the solution set—Eqs. (31) through (34), and Eqs. (38) and (39) for the NO + CO system; Eqs. (41) through (43) for the N₂O + CO system—cannot be treated as an explicit solution set since some parameters are not constants but depend on θ_{CO} and θ_N through ϵ_{CO} due to repulsive interactions among CO_a and N_a on the surface, as can be seen in Table 1. This situation can be handled very easily by determining the correct value of ϵ_{CO} through an iterative procedure.

Listed in Table 2 are the values of the nondimensional model parameters calculated from Table 1 with the correct values of ϵ_{CO} iteratively determined for both the isolated N₂O + CO system and the overall NO + CO system at 583 K. Note that the parameter values of β , r_2 , Γ_A , Γ_B , Γ_C , and Δ are not the same for both systems. This is physically related to the fact that the repulsive interaction among adsorbed species, as manifested through ϵ_{CO} in Table 2, is different for both systems due to different coverages of the surface species, as shown in Ta-

TABLE 3
Comparison of Surface Coverages and
Rate-Enhancement Factor (583 K)

Surface coverage	Isolated system	Overall system
θ_{CO}	0.880	0.376
$\theta_{\text{N}_2\text{O}}$	1.466×10^{-9}	5.072×10^{-7}
θ_v	0.120	0.274
θ_{N}	0.0	0.344
θ_{NO}	0.0	5.417×10^{-3}
Enhancement factor		
η	1.0	346

Note. $C_{\text{CO}} = C_{\text{N}_2\text{O}} = 400$ ppm was used for the isolated system; $C_{\text{NO}} = C_{\text{CO}} = C_{\text{N}_2\text{O}} = 400$ ppm was used for the overall system.

ble 3. The small value of Δ_0 compared with Δ_1 in Table 2 indicates that the inhibition effect due to surface coverages of reacting species is not so severe in the overall NO + CO system as in the isolated N₂O + CO system. Note that the two combined effects, large r_1 and small ratio of Δ_0 to Δ_1 , can synergistically enhance the reaction rate according to Eq. (46).

In view of the uncertainty about the exact value of $S_{\text{N}_2\text{O}}$, we have calculated the rate enhancement factor (η) as a function of $S_{\text{N}_2\text{O}}$. The value of $S_{\text{N}_2\text{O}}$ was varied in such a way that the product of $S_{\text{N}_2\text{O}}$ and k_6 remains constant at a given temperature. [We want to point out that the kinetic data by McCabe and Wong (13) provide a reliable value of the product of $S_{\text{N}_2\text{O}}$ and k_6 (i.e., $S_{\text{N}_2\text{O}}k_6$), even though the individual values of $S_{\text{N}_2\text{O}}$ and k_6 are still unknown. Thus, when the value of $S_{\text{N}_2\text{O}}$ is varied, it is imperative that the value of k_6 be varied in a compensating fashion in order to keep constant the value of $S_{\text{N}_2\text{O}}k_6$ determined by McCabe and Wong (13).] Note that the simultaneous variation of $S_{\text{N}_2\text{O}}$ and k_6 while keeping their product constant does not affect the rate of the isolated N₂O + CO reaction. For equivalent comparison $C_{\text{N}_2\text{O}}$ was assumed to be the same for both the overall system and the isolated system. The rate-enhancement factor calcu-

lated at 583 K under the conditions listed in Table 2 is shown in Fig. 2. It increases monotonically from 3 to 700 as $S_{\text{N}_2\text{O}}$ decreases from 1 to 0.001. Considering that the reasonable estimate of $S_{\text{N}_2\text{O}}$ is on the order of 10^{-3} as discussed earlier, we can expect from Fig. 2 the rate enhancement of two to three orders of magnitude for the intermediate N₂O + CO reaction in the overall NO + CO reaction system compared to the isolated N₂O + CO reaction. This makes the rate of the intermediate N₂O + CO reaction as fast as or even faster than the rate of the overall NO + CO reaction, since the rate of the NO + CO reaction at 583 K was reported to be approximately 240 times faster than the rate of the isolated N₂O + CO reaction (13).

Surface coverages of individual reacting species in both systems obtained at 583 K under the conditions listed in Table 2 can be directly compared in Table 3. In the isolated N₂O + CO reaction system, CO_a is the predominant surface species while the surface coverage by N₂O is negligibly small, in good agreement with McCabe and Wong (13). On the other hand, in the overall NO + CO reaction system, the dominating surface species are N_a and CO_a with nearly the same

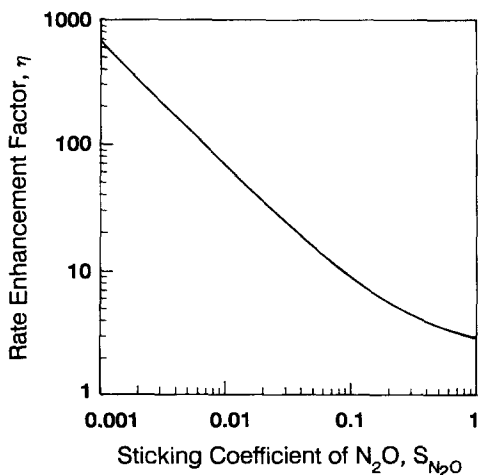


FIG. 2. Rate enhancement factor as a function of the sticking coefficient of N₂O.

TABLE 4

Comparison of Surface Coverage Expressions between Isolated System and Overall System

	Isolated system	Overall system
θ_{CO}	$\{(\beta + r_2)\Gamma_{\text{B}} - r_2\Gamma_{\text{C}}\}/\Delta$	$\{(\alpha + 2r_1)(\beta + r_2)\Gamma_{\text{B}} - r_1(\beta + 2r_2)\Gamma_{\text{A}} - r_2(\alpha + 2r_1)\Gamma_{\text{C}}\}/\{(\alpha + 2r_1)\Delta\}$
$\theta_{\text{N}_2\text{O}}$	Γ_{C}/Δ	$\{(\alpha + 2r_1)\Gamma_{\text{C}} + r_1\Gamma_{\text{A}}\}/\{(\alpha + 2r_1)\Delta\}$
θ_{v}	$(\beta + r_2)/\Delta$	$(\beta + r_2)/\Delta$
θ_{N}	—	$\{(r_1 - 1)(\beta + 2r_2 - 1) + r_2 - 1\}\Gamma_{\text{A}}/\{(\alpha + 2r_1)\Delta\}$
θ_{NO}	—	$(\beta + r_2)\Gamma_{\text{A}}/\{(\alpha + 2r_1)\Delta\}$

surface coverages. This large surface coverage of N_a and CO_a may have some connection to the formation of NCO species observed in many IR studies (e.g., 8, 25, 26). It is important to note in Table 3 that $\theta_{\text{N}_2\text{O}}$ in the overall NO + CO system is more than two orders of magnitude larger than that in the isolated N₂O + CO system, resulting in a large rate-enhancement factor. This increase of $\theta_{\text{N}_2\text{O}}$ in the NO + CO reaction system compared to the isolated N₂O + CO system is due to the production of N₂O_a on the surface via NO_a dissociation producing N_a and O_a [Eq. (3)] and the subsequent association of NO_a and N_a [Eq. (4)]. Note also that the vacant catalytic site (θ_{v}) available for adsorption and reaction is more than doubled in the overall NO + CO system compared to that in the isolated N₂O + CO system.

DISCUSSION

As shown earlier, the elementary surface processes occurring on the catalytic surface during the NO + CO reaction over noble metal catalysts are very complex, and the mathematical description of the system is highly nonlinear. It appears that this complex nonlinearity has been the major difficulty in developing an analytical solution for this system; to the best of our knowledge, there has been no analytical solution available so far, even though some numerical simulations of this system have been reported (7, 10).

With the belief that an analytical solution can give us better insight into the NO + CO

reaction system than the direct numerical simulation, we have developed a complete set of analytical solution for the overall NO + CO reaction system which includes the intermediate N₂O + CO reaction step. This solution set is in a very versatile form, so that it can also be used for the isolated N₂O + CO reaction system simply by changing a couple of parameter values. Results are summarized in Table 4 for ready comparison between the two systems. The idea was based on a quasilinear representation of the inherently nonlinear system by identifying a critical kinetic parameter that can be used to transform the kinetic model equations of the system into an optimization problem. The key to our success rests primarily on this critical parameter which was used as an optimization parameter (r_1). As the key parameter of the NO + CO reaction system, the optimization parameter implicitly carries the site-blocking effect due to adsorbed NO and nitrogen atoms which are absent in the isolated N₂O + CO system but present in the overall NO + CO system. This is why the geometric site-blocking effect due to NO_a and N_a is not shown explicitly in the expression for the surface coverages [i.e., Eqs. (31) through (34)], as normally expected in adsorption isotherms of the Langmuir type.

In our solution scheme, we have also introduced an inhibition function which can be used for both the overall and the isolated systems. This inhibition function is physically related to the effect of repulsive interactions among adsorbed CO_a and N_a spe-

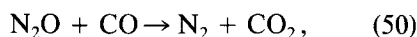
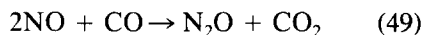
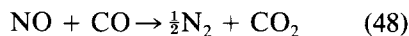
cies. Thus, it is important to recognize that, even if the form of this function remains identical for both systems, its numerical value can be quite different due to different surface coverages encountered in both systems.

Strictly speaking, the analytical solution obtained in this paper is valid only when $\delta\theta_N^2$ is much smaller than $(2\Gamma_C + \Gamma_A)$. In this regard, we want to point out that kinetic experiments for the NO + CO reaction over supported noble metal catalysts are generally performed at atmospheric total pressure with NO concentrations on the order of several hundred ppm, a typical level in automobile exhaust. Under these typical experimental conditions, the above condition [i.e., Eq. (22)] is always satisfied. Thus, the analytical solution developed in this paper can be used for practically all NO + CO kinetic experiments performed under atmospheric total pressure conditions. For UHV conditions, applicability of our solution should be checked by comparing the value of $(2\Gamma_C + \Gamma_A)$ with that of $\delta\theta_N^2$ shown in Fig. 1.

We have shown that the rate of the intermediate $N_2O + CO$ reaction during the overall NO + CO reaction can be as fast as, or even faster than, the overall NO + CO reaction, even though the isolated $N_2O + CO$ reaction is very slow. This finding has far reaching implications in our current understanding of the kinetic mechanism of the NO + CO reaction; it indicates that the $N_2O + CO$ reaction plays a very important role during the reduction of NO by CO over supported Rh catalysts. It also suggests that the suppression of product selectivity to N_2O formation observed at temperatures above 300°C during the NO + CO reaction (11, 13, 27) may not be due to the absence of the N_2O formation as was previously believed. It may very well be due to fast surface reaction of N_2O_a with CO_a immediately following the formation of N_2O_a . Our latest experimental data, to be published shortly, appear to support this speculation.

A further implication is that the overall reaction scheme proposed earlier for the re-

duction of NO by CO under most experimental conditions of practical interest (11), namely,



may probably be revised for high-pressure (i.e., atmospheric pressure) experimental conditions by eliminating Eq. (48). In other words, Eqs. (49) and (50) without the help of Eq. (48) can adequately describe the kinetics of NO reduction by CO under high-pressure conditions. There are two reasons behind this speculation. One reason is that the extent of N_2 desorption via recombination of two N_a is negligible under the high-pressure reaction conditions, as shown earlier in Eq. (22). The other is that Eqs. (49) and (50) reduces to Eq. (48) when the intermediate $N_2O + CO$ reaction is sufficiently fast.

SUMMARY AND CONCLUSIONS

Since we first observed the participation of the $N_2O + CO$ reaction as an *intermediate* reaction step during the NO + CO reaction over supported Rh catalysts (11), it has been reported in the literature that the rate of the $N_2O + CO$ reaction as an *isolated* reaction is very slow compared to the rate of the NO + CO reaction. Unfortunately, this latter finding appears to have led many researchers to the false conclusion that the contribution of the $N_2O + CO$ reaction to the overall NO + CO reaction is negligible. The kinetic analysis based on elementary surface processes presented in this paper shows a clear distinction between the rate of the $N_2O + CO$ reaction as an *intermediate* reaction and that as an *isolated* reaction. Results of comparative kinetic analysis have indicated that the formation of N_2O and its subsequent reaction with CO are very important intermediate reaction steps in the reduction of NO by CO on Rh/Al₂O₃ catalysts. In view of the similar behavior in the formation of the intermediate N_2O during

NO decomposition over noble metal catalysts (28), we speculate that the same is true for other noble metal catalysts such as Pt. Thus, our discovery of this analytical solution promises to provide a better understanding of the $NO + CO$ reaction kinetics for automotive exhaust emission control using the noble metal catalysts. More specific findings are listed below.

1. The rate of the $N_2O + CO$ reaction as an intermediate reaction step in the overall $NO + CO$ reaction system can be much faster than the rate of the $N_2O + CO$ reaction as an isolated reaction. The amount of this rate enhancement is estimated to be two to three orders of magnitude.

2. The rate enhancement can be explained by the combined effect of increased N_2O surface coverage and the decreased inhibition effect on the catalytic surface in the overall $NO + CO$ system compared with those in the isolated $N_2O + CO$ system. The former effect is due to the contribution of surface reactions leading to the production of adsorbed N_2O , while the latter effect is due to the increased repulsive interactions among adsorbed CO and nitrogen species creating more vacant catalytic sites available for N_2O adsorption and dissociation.

3. As a result of this rate enhancement, the rate of the intermediate $N_2O + CO$ reaction can be as fast as or even faster than the rate of the overall $NO + CO$ reaction. This then suggests that the $N_2O + CO$ reaction is a very important intermediate step in the overall $NO + CO$ reaction over supported noble metal catalysts.

One may argue that there is a possibility of the exact magnitude of the rate enhancement factor being larger or smaller than our present estimation, depending upon the exact value of the sticking coefficient of N_2O , as shown in the sensitivity analysis (Fig. 2). However, our latest experimental evidence supports the above conclusions in general, indicating that the value of S_{N_2O} used in this paper is a reasonable estimation for the purpose of illustrating the rate enhance-

ment of the intermediate $N_2O + CO$ reaction in the overall $NO + CO$ reaction system. A report on the experimental verification of this kinetic theory will be published shortly.

APPENDIX: NOMENCLATURE

C_i	gas phase concentration of species i , mol/cm ³
f_i	one fourth the average molecular speed of species i , cm/s
H	a unit vector defined by Eq. (26)
k_1	adsorption rate constant of NO, (cm ³ /mol) s ⁻¹
k_{-1}	desorption rate constant of NO _a , s ⁻¹
k_2	adsorption rate constant of CO, (cm ³ /mol) s ⁻¹
k_{-2}	desorption rate constant of CO _a , s ⁻¹
k_3	dissociation rate constant of NO _a , s ⁻¹
k_4	association rate constant between NO _a and N _a , s ⁻¹
k_5	adsorption rate constant of N ₂ O, (cm ³ /mol) s ⁻¹
k_{-5}	desorption rate constant of N ₂ O _a , s ⁻¹
k_6	dissociation rate constant of N ₂ O _a , s ⁻¹
k_7	desorption rate constant of N _a , s ⁻¹
k_8	rate constant of CO oxidation, s ⁻¹
K_i	adsorption equilibrium constant of species i , cm ³ /mol
M	(3 × 4) kinetic matrix for $NO + CO$ reaction system defined by Eq. (24)
M_i	molecular weight of species i
r_1	dimensionless NO dissociation rate constant defined in Eq. (18)
r_2	dimensionless N ₂ O dissociation rate constant defined in Eq. (18)
R_g	ideal gas constant
R_i	rate of the isolated $N_2O + CO$ reaction, s ⁻¹
R_0	rate of the intermediate $N_2O + CO$ reaction in the overall $NO + CO$ reaction system, s ⁻¹
S	catalytic surface site
S_i	sticking coefficient of adsorption for species i
T	temperature, K
<i>Greek Letters</i>	
α	dimensionless NO _a desorption rate constant defined in Eq. (17)

- β dimensionless N_2O_a desorption rate constant defined in Eq. (17)
- γ dimensionless NO_a dissociation rate constant defined in Eq. (17)
- Γ_i dimensionless gas phase concentration of species i defined in Eq. (15)
- δ dimensionless N_a desorption rate constant defined in Eq. (17)
- Δ inhibition function defined by Eq. (35)
- ε_{CO} change in activation energy for CO_a desorption due to repulsive interaction among CO_a and N_a on the surface, cal/mol
- ε_N change in activation energy for N_a desorption due to repulsive interaction among N_a on the surface, cal/mol
- η rate enhancement factor defined by Eq. (46)
- θ_i surface coverage of species i
- Θ a vector of surface coverage defined by Eq. (25)
- σ area occupied surface metal atoms, cm^2/mol

Subscripts

- a adsorbed state
- A NO species
- B CO species
- C N_2O species
- i chemical species ($i = NO, CO, N_2O,$ or N)
- v vacant surface site

REFERENCES

- Voltz, S. E., Morgan, C. R., Liederman, D., and Jacob, S. M., *Ind. Eng. Chem. Prod. Res. Dev.* **12**, 294 (1973).
- Oh, S. H., and Carpenter, J. E., *J. Catal.* **101**, 114 (1986).
- Taylor, K. C., in "Catalysis: Science and Technology" (J. R. Anderson and M. Boudart, Eds.), Vol. 5. Springer-Verlag, Berlin, 1984.
- Campbell, C. T., and White, J. M., *Appl. Surf. Sci.* **1**, 347 (1978).
- Taylor, K. C., and Schlatter, J. C., *J. Catal.* **63**, 53 (1980).
- Dubois, L. H., Hansma, P. K., and Somorjai, G. A., *J. Catal.* **65**, 318 (1980).
- Hecker, W. C., and Bell, A. T., *J. Catal.* **84**, 200 (1983).
- Hecker, W. C., and Bell, A. T., *J. Catal.* **85**, 389 (1984).
- Root, T. W., Schmidt, L. D., and Fisher, G. B., *Surf. Sci.* **150**, 173 (1985).
- Oh, S. H., Fisher, G. B., Carpenter, J. E., and Goodman, D. W., *J. Catal.* **100**, 360 (1986).
- Cho, B. K., Shanks, B. H., and Bailey, J. E., *J. Catal.* **115**, 486 (1989).
- Cho, B. K., *J. Catal.* **131**, 74 (1991).
- McCabe, R. W., and Wong, C., *J. Catal.* **121**, 422 (1990).
- Belton, D. N., and Schmiege, S. J., unpublished results.
- Solimosi, F., and Sarkany, J., *J. Appl. Surf. Sci.* **3**, 68 (1979).
- Tompkins, F. C., "Chemisorption of Gases on Metals." Academic Press, London, 1972.
- Avery, N. R., *Surf. Sci.* **131**, 501 (1983).
- Daniel, W. M., Kim, Y., Peebles, H. C., and White, J. M., *Surf. Sci.* **111**, 189 (1981).
- Shi, S.-K., and White, J. M., *J. Chem. Phys.* **73**, 5889 (1980).
- Fisher, G. B., and DiMaggio, C. L., unpublished results.
- Barker, F. G., and Gasser, R. P. H., *Surf. Sci.* **39**, 136 (1971).
- West, L. A., and Somorjai, G. A., *J. Vac. Sci. Technol.* **9**, 668 (1972).
- Weinberg, W. H., *J. Catal.* **28**, 459 (1973).
- Amundson, N. R., "Mathematical Methods in Chemical Engineering." Prentice-Hall, Englewood Cliffs, NJ, 1966.
- Kiss, J., and Solymosi, F., *Surf. Sci.* **135**, 243 (1983).
- Dictor, R., *J. Catal.* **109**, 89 (1988).
- Oh, S. H., *J. Catal.* **124**, 477 (1990).
- Cho, B. K., and Stock, C. J., in "1986 Annual Meeting of American Institute of Chemical Engineers, Miami Beach, FL, Nov. 1986."